Usage Report for Fiscal Year 2019

Project Title: Transport properties of self-propelled micro-swimmers

Name: Dr. Franco Nori (team leader)
Dr. Pulak Kumar Ghosh

Laboratory at RIKEN: Theoretical Quantum Physics Laboratory

I. Background And Purpose:

Self-propelling Janus particles (JPs), the most common class ofartificial microswimmer, have been the focus of widespread attention over thelast two decades due to their emerging applications in nano-technology andmedical sciences [1-3]. Such particlesare made by coating one hemisphere with catalytic or photo-sensitive ormagnetic materials. Under appropriateconditions, one hemisphere undergoes physical or chemical changes withrespect to the other, thus producing some local gradient in the suspensionfluid (self-phoresis). This strategy allows artificial swimmers topropelthemselves by harvesting energy from their environment.

Thanks to their self-propulsion mechanism and in contrast to their passivepeer, artificial swimmers can diffuse orders of magnitude fasterare capable of performing autonomous motion in periodicstructures with broken spatial symmetry andexhibit other peculiar transport properties.Inspired by these unique transport features, researchers aimto design customized JPs to be used, for instance, as ``nano-robots'' capableof performing accurate mechanical operations. Additional promisingtechnological applications have also been proposed. Among the most appealing ideas beingpursued, we mention here the recent attempt to power passive particlesthrough the self-propulsion mechanism of intermediary active particlesto be used ascontrollable stirrers.

Adding a relativelysmall fraction of highly motile microswimmers to a suspension of less motilemicroswimmers can considerably enhance the overall motility of the mixture due stirring effect.This effect easily can be demonstrated in the presence of inertia. But what will happen to overdamped or mass-less particles? This limitcorresponds to low Reynolds numbers, a hydrodynamic regime that applies tomost microswimmers investigated in the literature, both biological andartificial. This raises a problem, because, the velocitydistribution of massless particles is mathematically ill-defined. Thus, the host-guest motility transfer due to stirring effect cannot be perceived in the overdamped regime. To avoidthis difficulty, in our simulations we computed an alternative motility quantifier in the overdamped limit, namely the effusion rate of the activeJPs through a narrow pore of the simulation box.

Mixtures of interacting active particles (either of thesame or different kinds) behave quite differently in many ways. For dilutesolutions, particles interact via long-range hydrodynamic flows generated byactive particles and the short-range interactions can be safely ignored. However, transport properties of dense mixtures are mostlydominated by the short-range interactions, which are responsible for avariety of cluster and pattern formation processes reported in the recent literature.

Our simulation of binary active mixtures shows that adding a fraction ofactive microswimmers, such as self-propelled JPs, to a suspension of passivecolloidal particles, results in a motility increase of the latter species. However, adding a small fraction of more active particles to a suspension ofless active microswimmers, results in a non-trivial behavior, whereby theadded species appears to enhance the motility of the host species. Such amechanism can be controlled by tuning the parameters ofthe guest species,e.g., the intensity of light in the case of

light-induced JP using laser beam, near-infrared light or visible light.

Note that in an previous occasion (fiscal year 2017) we worked on the motility transfer in binary mixture that focus on the particles with inertia (that is stirring effect works there). Simulation results in presented this report (produced in fiscal year 2019) explore motility transfer of highly damped particles, where stirring effect does not work and motility transfer is a non-trivial effects.

2.Model:

Let us consider a two-dimensional system consisting of two types of JPs with different self-propulsion speeds in a thermal bath: N_w with speed v_w and N_s with speed v_s, For very short distances they interact with each other via a truncated Lennard-Jones potential,

$$V_{ij} = 4\varepsilon\left[\left(\frac{\sigma}{r_{ij}}\right)^{12} - \left(\frac{\sigma}{r_{ij}}\right)^{6}\right], \text{ if } r_{ij} \le r_m$$

$$= 0 \text{ otherwise,}$$

where r_m locates the potential minimum and $\sigma = 2r_0$. The corresponding Langevin equations, describing motion of the particles in the mixture in the highly damped situation are,

$$\dot{x}_i = \sum_j F_{ij}^x + v_0 \cos\phi_i + \sqrt{2D_0}\,\xi_i^x(t) \text{ -- (1)}$$

$$\dot{y}_i = \sum_j F_{ij}^y + v_0 \sin\phi_i + \sqrt{2D_0}\,\xi_i^y(t) \text{ -- (1)}$$

$$\dot{\theta}_i = \sqrt{2D_\theta}\,\xi_i^\theta(t). \quad \text{---------- (3)}$$

The particle with instantaneous position $\{x_i, y_i\}$ diffuses in the force field under the combined action of self-propulsion and equilibrium thermal fluctuations. $\{\xi_{x_i}, \xi_{y_i}\}$ are components of random thermal fluctuation, responsible only for translational diffusion, is modeled by a Gaussian white noises with,

$$\langle \xi_i^q(t) \rangle = 0$$

$$\langle \xi_i^q(t)\xi_j^{q'}(0) \rangle = 2\delta_{ij}\delta_{qq'}\delta(t)$$

Where q or q' = {x, y}. The thermal noise strength, $D_0 = k_BT/\gamma$ can be estimated by measuring the translational diffusion of a free JP in the bulk in the absence of propulsion.

The propulsion velocity v_i, with modulus v_0, directed making an angle ϕ_i with respect to the laboratory x-axis. Due to rotational diffusion of the particle, θ_i changes randomly, which can be described as a Wiener process, as described in Eq.(3), with following statistical properties

$$\langle \xi_\theta(t) \rangle = 0$$

$$\langle \xi_\theta(t)\xi_\theta(0) \rangle = 2\delta_{ij}\delta(t)$$

The rotational diffusion constant D_θ is related to the viscosity (η_v) of the medium, temperature (T) and size of the particle. For spherical particle with radius a, rotational diffusion constant can be expressed as $D_\theta = k_BT/8\pi\eta_v r_0^3$. However, rotational diffusion may contain contribution of gradient fluctuations that are very much related to mechanism of acquiring self-propulsion. The mechanisms and origins of the translational and rotational diffusion may not be the same. Thus, D_0, v_0, and D_θ can be treated as independent model parameters.

We numerically integrated Eqs. (1-3) using a standard Milstein algorithm to obtain effusion rates of the both mixture species. The numerical integration was performed using a very short time step, 10^{-6} -10^{-7} to ensure numerical stability. At t = 0, the particles were uniformly distributed in the box with randomorientation. To keep the number density of both species constant, a particle of the same species wasre-injected with random position and orientation inside the box,whenever one had escaped through the pore. The datapoints reported in the figures shown here,have been obtained by ensembleaveraging over a minimum of 10,000 trajectories.

Result and discussions:

The effusion rate has been studied in depth to characterize classical transport inconstrained geometries [4]. We define the effusion rate of the

strong (*s*) [*weak (w)]* JPs, E_s (E_w), as the number of *s* (*w*) particles exiting the simulation box per unit time.In the case of a single-component system, we denote the effusion rate by E_m.

Effusion of non-interacting species: Let us consider the effusion rate $E_m(0)$ of a single species of non-interacting JPs. In Fig.1(a) we plotted a fewcurves $E_m(0)$ versus v_0 for different values of D_θ. For $v_0 \rightarrow 0$ the effusion is controlled by thermal motion and, asexpected, is insensitive to v_0. Effects due to self-propulsion becomeappreciable only for values of v_0 larger than the particles thermal speed. Beyond this critical value, the effusion rate grows first quadratically with $v_0$and then saturates toward an asymptotic value.

The rising branches occur for $l_\theta > x_L, y_L$. Indeed, for veryshort rotational relaxation times τ_θ when it can safely beassumed that particles diffuse in a thermal bath with effective constant D_{eff} the effusion rate through a narrow pore of effective width much smaller than the confining box.

$$E_i = \pi \rho_i D_{\text{eff}} \left[\ln \left(\frac{x_L + y_L}{\Delta} \right) \right]^{-1}$$

Here, the suffix i refers to either s or w, ρ_i denotes the numberdensity of the mixture component i, and D_{eff} is now, $D_0 + v_0^2/2D_\theta$ – see Eq.(5). This estimate for Ei(0) agrees fairly closely withthe simulation results reported in Fig. 5(a). In the opposite rotationalregime, when $l_\theta >> x_L, y_L$, the slow direction changes ofthe self-propulsion velocity tends to suppress the particles effusionthrough the pore. Assuming that τ_θ is much larger than anyother system time scale, the effusion rate can be approximatedby,

$$E_i(0) \approx x_L y_L \rho_i D_\theta / \pi$$

This asymptotic estimate has been marked in Fig. 5(a) by horizontalarrows.

The effusion rate of interacting self-propelling particles with $\varepsilon > 0$ is plotted in the inset of Fig. 5(a). This figure shows the v_0-dependence of the effusion rate relative to the corresponding ratein the absence of interaction, $E_m(\varepsilon) = E_m(0)$, for several values of D_θ. The system we simulated here was quite dense ($\phi = 0.66$),so that the self-propulsion mechanism becomes strongly constrained, being $l_s << l_\theta$. Like in non-interacting systems, the effusionrate is insensitive to self-propulsion with low v_0. Moreremarkably, with increasing v_0 the relative effusion decreases.

We attributed this result to the jamming of the interactingparticles caused by self-propulsion near thebox walls. Snapshots of the mixture configurations [Fig 2 and Fig.3(b) (inset)] corroborate this assertion. Jamming effect gets noticeable as soon as theself-propulsion length becomes larger than the confining box.

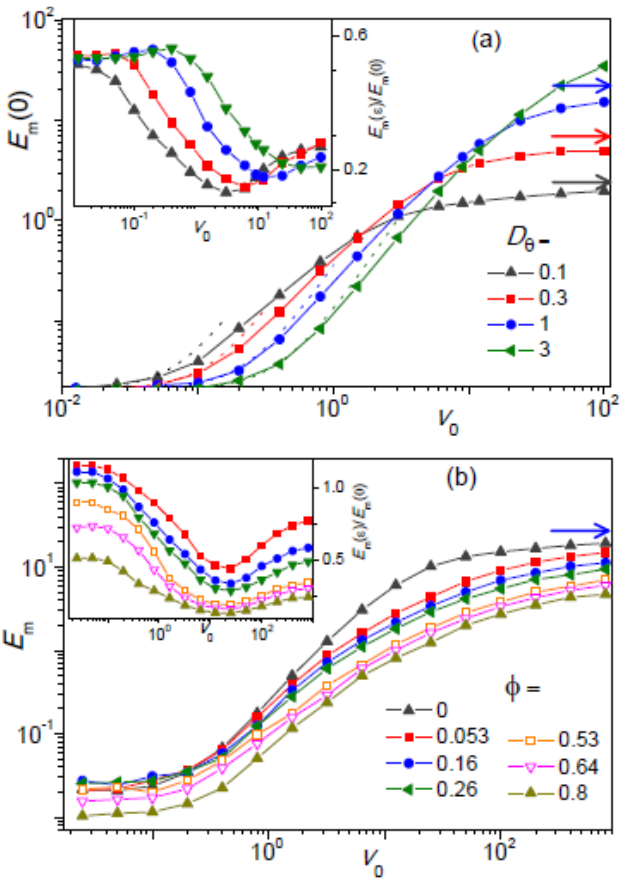

Fig1: (a) Effusion rate $E_m(0)$ of non-interacting JPs with $\varepsilon = 0$, as a function of the self-propulsion speed, v_0, for different rotational diffusion coefficient D_θ. Dotted lines are the predictions based on Eq. (16). Horizontal arrows indicate the corresponding rate upper bound, Eq. (17), for large $\tau_\theta = 1/D_\theta$. Inset: the effusion rate ratio $E_m(\varepsilon)=E_m(0)$for $\varepsilon = 0.1$ and

different D_θ (see legends). (b) Effusion rate $E_m(\varepsilon)$ of interacing self-propelled particles versus v_0 for e = 1 and different packing fraction f. Inset: $E_m(\varepsilon)=E_m(0)$ versus v_0 for the same set of parameter as the main panel. Other simulation parameters for main panels and inset: $x_L = y_L = 10$; $\Delta = 0.5$; $r_0 = 0.5$; $D_0 = 0.03$; $N_m = 80$.

More remarkably, excluded volume effect become apparent for $v_0 \rightarrow 0$; the interacting particles become more effusivethan the non-interacting ones. In a dilute solution, thiseffect persists until self-propulsion length grows larger thanthe average inter-particle spacing. This explains why, in thepresence of strong self-propulsion, the computed effusion ratiosstill grow with v_0, though quite slowly. Therefore, the appearance of such an effect and minima of $E_m(\varepsilon)/E_m(0)$ versus v_0 are inversely related to the rotationaldiffusion [see inset of Fig. 1(a)]. By the same token, one expectsthat both decaying and

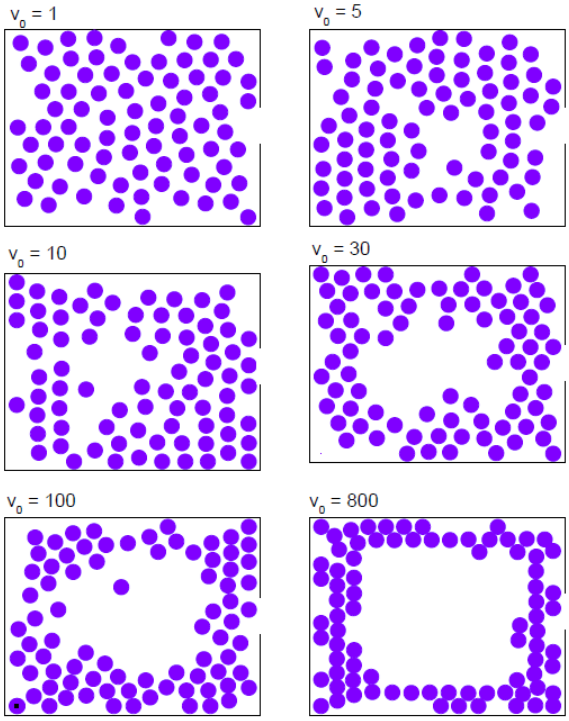

Fig2: Snapshot of phase points of interacting JPs for different self-propelled velocity v_0 and other parameters ε =1, confining length, $x_L = y_L$ =1 0, opening size $\Delta = 0.5$, particle radius $r_0 = 0.5$, $D_0 = 0.03$, and total particles $N_t = 80$.

raising branches of the curves $E_m(\varepsilon)/E_m(0)$ versus v_0 are quite insensitive to the packing fraction,ϕ, in agreement with the data plotted in the inset of Fig.1(b). In the very strong self-propulsion regime, both $E_m(\varepsilon)$ and $E_m(0)$ tend to saturate [see Fig. 1(b)]. However, $E_m(\varepsilon)$ saturates at larger v_0 values than in the non-interacting case.A plausible explanation is suggested by a comparison of themixture snapshots [see Fig.2]. The particles far away from the walls aremore mobile and contribute more to the effusion rate; theyare not jammed against the walls and "see" a larger opening width to compartment-size ratio, D/y_L. In contrast, particlesjammed against the walls tend to clog the box opening. However, the fraction of the more mobile particles drops fast withincreasing v_0, thus leading to plateaus of effusion rate in thelimit v_0 Figure 1(b) shows that the clogging mechanism works evenat low packing fraction, though its impact on effusion is reduced.

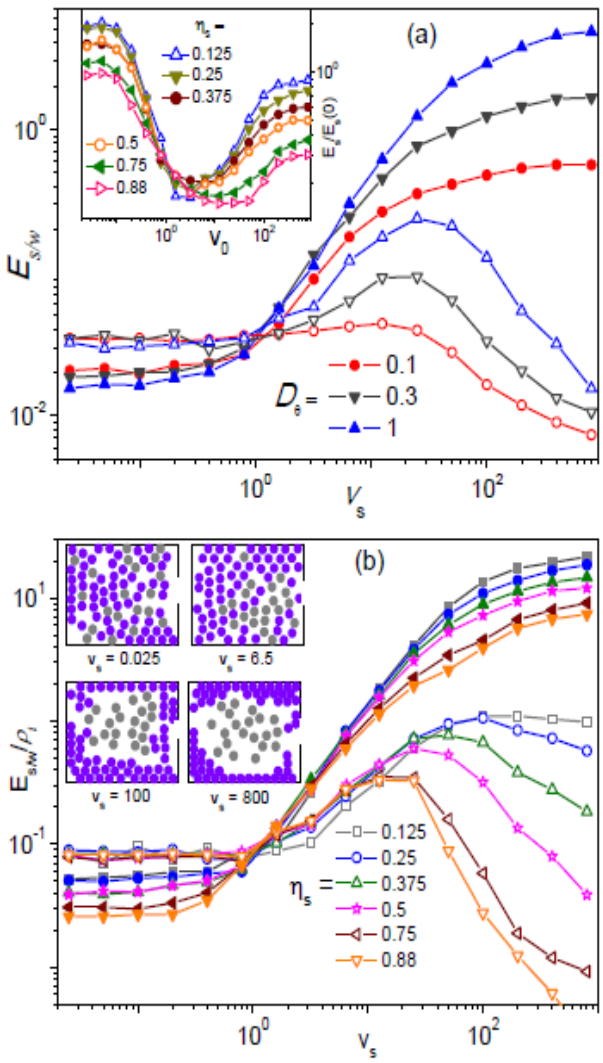

Fig3: (a) Effusion rates E_s(filled dots) and E_w(empty dots) versus vs for binary mixture with $\eta_s = 0.5$ and different values of D_θ (see legends). Inset: Effusion ratio of stronger component, $E_m(\varepsilon) = E_m(0)$versus $v_0$for different η_s and $D_\theta = 1$. (b) Effusion rates E_s (filled dots) and E_w (empty dots) versus vs in a binary mixture for $D_\theta = 1$ and different η_s(see legends). Inset: Snapshot of binary mixture with $\eta_s = 0.75$, $D_\theta = 1$and different v_s [0.025 (top-left), 6.5 (top-right), 100 (bottom-left), and 800 (bottom-right)]. Other simulation parameters for main panels and insets:$v_w = 1$; $\varepsilon = 1$, $x_L = y_L = 10$; $\Delta = 0{:}5$; $r_0 = 0.5$; $D_0 = 0{:}03$; $N_m = 80$.

Figure 3(a) illustrates the dependence of the effusion rates Eof the two active mixture components on their self-propulsion parameters,v_0 and D_θ. The mixture is of 1:1 molar ratio of strongly (s) and weakly (w) active particles. In Fig. 3(b), we examine the consequences of gradually increasingthe fraction of guest particle for different values of their self-propulsionspeed, v_s. While all effusion plots exhibit the same general behavior as in Fig 3(a), a few additional features areremarkable:

(i) The effusion rate of the strongly active JPs keeps increasing,but more slowly than $E_m(0)$ in Fig. 1(a), due to their interactionwith the less active JPs. In such a limit, the mostactive particles tend to push the less active ones against thebox walls. Moreover, like in one component systems, cloggingeffects have great impact on the effusion of both the weak andstrong active components.

(ii) On the contrary, the effusion rate of the weak JPs remainsunchanged for v_s up to v_w; upon further increasing v_s, it goes through a maximum in correspondence with themechanism of effective motility transfer. Again, for very large self-propulsion, $v_s >> x_L D_\theta$; $y_L D_\theta$, strongly active JPs jamagainst the container walls, thus pushing the weaker JPs inside [see snapshots of Fig 3(b) and Fig, 2]. Accordingly, the weaker JPs have a little chance to escapethrough the opening so that effusion is drastically suppressed.

Moreover, no decaying branch of E_w vs. v_s is detectable at low η_s. This happens because very few strong JPscannot possibly confine all weak particles in the box' interior.

In conclusion, we stress that adding a small amount ofstrongly active JPs does suffice to enhance the effusion ofsluggish active JPs, but an excess of them can produce the opposite effect! We also remind that, as illustrated by our simulation snapshots, the two components of an active binarymixture can separate into two distinct phases, when theself-propulsion length of one is much larger than the size ofthe container and the other one much shorter, that is, for $v_s/D_\theta >> x_L; y_L >> v_w/D_\theta$. However, phase segregation shouldbe avoided for better motility transfer.

As shown in figure 1(b), there is a window of the tunable v_s,where the effusion rate of the weak particles becomes enhanced by 2 to 7 times, depending on their rotational relaxation time andcomposition of binary mixture. Also, the span of this window issensitive to the persistence length of self-propelled motion. This striking result confirms that, even in the absence of inertia, themotility of the more active microswimmers can be effectively transferred to the less active microswimmers. In our numerical analysis we assumed the pore to be centeredin one side of a square-shaped simulation box. However, slidingboundary conditions as the JPs move against the cavity walls,can affect their average effusion rate. Our simulation shows thatthis may become an issue only at zero temperature. As a matterof fact, thermal fluctuations assist the escape mechanism by enhancingparticle diffusion along the boundaries, thus suppressingpossible effects related to the cavity geometry and the actual porelocation. To verify this point, we simulated the effusion rate (not shown) for a modified box geometry, whereby the escape porewas moved toward one corner; for the simulation parameters of Fig. 1 we detected no

appreciable variations of the relevant effusionrates.

***

In addition to the research works described above, we are still working on other issues from last year's in particular diffusion control autocatalytic reactions.

V. Future plan

In the next fiscal year, we plan to explore the following issues:

(i) *Cooperativity in binary mixture of two sort of Janus particles*.

Our simulation results in binary mixture suggested that motility transfer in the overdamed regime associated with non-trivial dynamics of weak and strong JPs. We recognized some parameters regime of self-propulsion, where totally different effusion rate through motility transfer is observed. Large variation of effusion associated to change in spatial distribution of phase points, some of which show very crowded and uncooperative motions, while others seem to act as one resulting in better *cooperativity*. Now key issue we want to explore is the degree of cooperativity and its functional dependence on self-propulsion properties of both type of species in binary mixture. In general, cooperativity is quantify by estimating the following quantity.

$$N_X^{Co}(t) = 1 + \frac{\sum_{i \neq j} \langle X_i X_j \rangle}{\sum_i \langle X_i \rangle}$$

Where, $X_i(t) = r_i(t) - r_i(0)$, is the displacement of the i-th particle over time t. For uncorrelated motion, the above quantifier is one. Positive or negative value associated with some type of correlated motion. To understand in more detail the effects of correlated movement, in addition to the above quantifiers we also want to calculate pair distance and cooperativity of nearest neighbor particles.

(ii) *Escape kinetics of self-propelled Janus particles from circular cavity:*

Diffusion is the ubiquitous mechanism for intercellular transport of key bio-molecules that trigger many cellular functions, like cross-membrane ion-current, chemical balance, neuronal signaling etc. The transporting particles diffuse through narrow openings in an impermeable wall and reach at small target. The stochastic escape processes actually play the central role in governing time scale of many cellular functions. The rate of these significant events is largely dictate by geometry of cellular structures in addition to other factors (like, density gradients, temperature, solvation , pH etc) . Therefore, it is desirable to have detailed knowledge about escape rate to gain control over cellular function by tuning external parameters.

In the next, fiscal year we plan to numerically explore narrow escape kinetics for both normal and active Brownian particles. Active Brownian particles, the most fascinating ones are Janus particles, nowadays are designed to use them as a tracer for targeted drug delivery. Thus, the knowledge about their escape processes is of paramount interest. To be specific, here we want to explore escape processes (from circular cavity, see Fig.4) of both normal and active particles through single and/ormultiple small openings. We want to understand how the time correlation of the persistent Brownian motion of a JP affects its mean first passage time through one or more cavity openings.

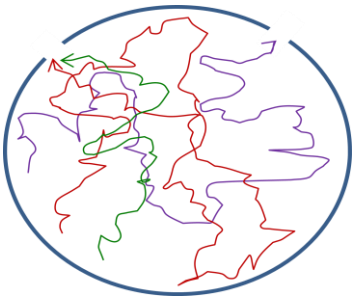

Fig.4: Schematic of some trajectories for Brownian particle in a circular cavity escaping through a very narrow opening.

***

To addressthe above-mentioned issues we will implement and the numerical scheme mentioned in Sec. III.

Currently, I have a "Quick Use" user account and I would like to get extension of computation facilities for next usage term (up to 31st March 2021) under the same user category.

VI. References

[1]S. Jiang and S. Granick (eds.), Janus Particle Synthesis, SelfAssembly and Applications (RSC, Cambridge, 2012).

[2] C. Bechinger, R. Di Leonardo, H. Löwen, C. Reichhardt, G. Volpe, and G. Volpe, Active particles in complex and crowded environments, Rev. Mod. Phys., 2016, 88, 045006

[3] P. K. Ghosh, V. R. Misko, F. Marchesoni, and F. Nori,Phys. Rev. Lett. **110**, 268301 (2013).

[4] D. Holcmanand, Z. Schuss, Stochastic Narrow Escapein Molecular and Cellular Biology (New York, Springer, 2015).

Fiscal Year 2017List of Publications Resulting from the Use of the supercomputer

[Publication]

T. Debnath, P. K. Ghosh, Y. Li, F. Marchesoni, and F. Nori, 'Active Diffusion Limited Reactions', The Journal of Chemical Physics , vol-150, article no. -154902, 15 April 2019 ; doi: 10.1063/1.5081125

[Proceedings, etc.]

None

[Oral presentation at an international symposium]

None

[Others (Press release, Science lecture for the public)]

None